Geckobot: A Gecko Inspired Climbing Robot Using Elastomer Adhesives

Ozgur Unver
Department of Mechanical Engineering
Carnegie Mellon University
422 Scaife Hall, 5000 Forbes Avenue
Pittsburgh, PA 15213
ounver@andrew.cmu.edu

Ali Uneri, Alper Aydemir
Mechatronics Department
Sabanci University
Istanbul, Turkey
aliu@su.sabanciuniv.edu
osmana@su.sabanciuniv.edu

Metin Sitti
Department of Mechanical Engineering
Carnegie Mellon University
315 Scaife Hall, 5000 Forbes Avenue
Pittsburgh, PA 15213
msitti@andrew.cmu.edu

***Abstract*— In this paper, the design, analysis, and fabrication of a gecko-inspired climbing robot are discussed. The robot has kinematics similar to a gecko's climbing gait. It uses peeling and steering mechanisms and an active tail for robust and agile climbing as a novelty. The advantage of this legged robot is that it can explore irregular terrains more robustly. Novel peeling mechanism of the elastomer adhesive pads, as well as steering and stable climbing using an active tail are explored. The design, fabrication, analysis and test of the robot are reported. Experimental results of walking and climbing up to 85° sloped acrylic surfaces as well as successful steering and peeling mechanism tests are demonstrated. The potential applications foreseen for this kind of robots are inspection, repair, cleaning, and exploration.**

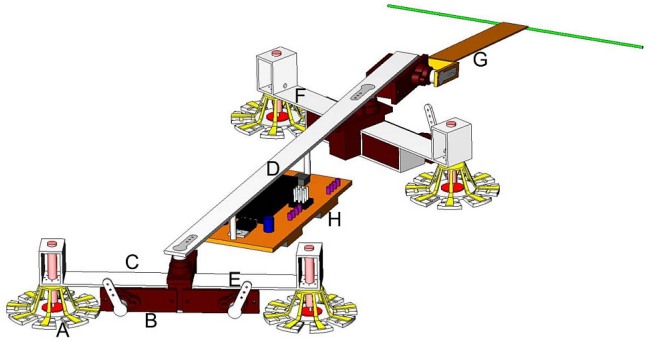

Fig. 1. Geckobot CAD drawing, A: Adhesive footpads, B: Servomotors, C: Front legs, D: Waist, E: Servomotor arm, F: Rear legs G: Active tail, H: Onboard components.

I. Introduction

Surface climbing robots have enabled robotic applications in complicated environments such as vertical or 3-D walls, ceilings, space shuttle outer surfaces, and volcanoes. They have been widely used for inspecting nuclear power plants [1], labeling oil tank volume scale [2], cleaning [3], sand blasting [4], and painting [5]. Other applications include building repair and maintenance, search and rescue, and toys. Recently, there has also been interest in using climbing robots to inspect and repair space vehicles.

Three general types of attachment mechanisms have been studied and developed. The most common type is suction adhesion, where the robot carries an on-board pump to create a vacuum inside cups which are pressed against the wall or ceiling [6], [7]. This type of attachment has some drawbacks associated with it. First, the suction adhesion mechanism requires time to develop enough vacuum to generate sufficient adhesion force. This delay reduces the speed at which the robot can move. Another issue is that any gap in the seal can cause the robot to fall. This drawback limits the suction adhesion mechanism to relatively smooth, non-porous, non-cracked surfaces. In addition, power consumption is too high during attachment. Finally, the suction adhesion mechanism relies on the ambient pressure to stick to a wall, and therefore it is not useful in space applications since the ambient atmosphere in space is essentially zero.

The second common type of adhesion mechanism is magnetic adhesion. Magnetic adhesion has been implemented in wall climbing robots for specific applications such as nuclear facility inspection [8], [9]. In specific cases where the surface allows, magnetic attachment can be highly desirable for its inherent reliability. Despite that, magnetic attachment is useful only in specific environments where the surface is ferromagnetic; hence, for most applications it is not suitable. In addition, the power consumption of magnetic adhesion could be extremely high.

The third type of adhesion mechanism is grasping technique, which requires holds, spines or grooves to grasp and pull the whole body upwards [10], [12]. For rough surfaces, this is a powerful technique. However, if the surface is flat and smooth, this method cannot be applied. Moreover, climbing down is challenging for this method.

As a novel recent attachment mechanism, passive attachment mechanisms have been proposed as robust techniques for climbing recently. The *Tokay gecko*, for example, can weigh up to 300 grams and reach lengths of 35 cm yet is still able to run inverted and cling to smooth walls using *fibrillar dry adhesives* in their footpads. Similar adhesive pads are aimed to have the Geckobot agile movements and robust climbing performance as geckos [11]. A Geckobot is designed to use a gecko-inspired synthetic dry adhesive, which does not need energy to stay on the surface or pressure differences to climb eventually. In addition, climbing can be achieved not only with gecko

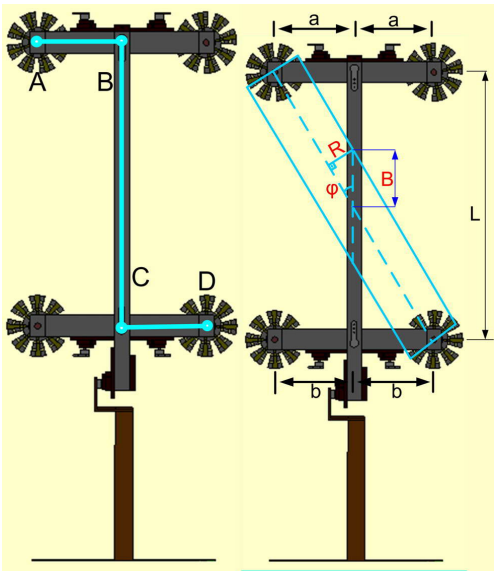

Fig. 2. Four-bar mechanism of the Geckobot (left image), The safety region of the Geckobot (right image).

inspired fibrillar dry adhesives but also with flat elastomers. The novelty of this work is *gecko-inspired gait* of the Geckobot to develop a methodology for inspired *active tail* based robust attachment, *steering* for high maneuverability, and optimal *peeling* mechanisms for power efficient detachment.

II. Geckobot Design

This paper aims to design a gecko-inspired robot that can walk, climb, and steer robustly and power efficiently as shown in Fig. 1. In order to achieve efficient wall climbing, the robot should be able to change its orientation and move in all directions. For climbing robots, to improve their climbing ability and to minimize power consumption, peeling mechanism and adhesive characteristics are very crucial. Peeling is a very crucial and challenging task for climbing robots to improve their climbing ability and to minimize power consumption. For autonomous performance, the source of energy, microprocessor, actuators and sensors have to be placed on the robot.

A. Walking on a Flat Surface

The robot is kinematic similar to a four-bar mechanism as shown in Fig. 2a. AB, BC, CD and ground are four linkages when front right and rear left feet are detached during walking and the circles on the lines illustrate the joints. Geckobot sequentially pulls two diagonally opposed feet up and by using motors on the four-bar mechanism pushes itself forward. Then, the feet that are aloft are attached back to the ground and the opposite feet are lifted up for the next forward motion. The aim is to keep the center of gravity (CG) inside the safety region (SR) shown in Fig. 2b, which is formed by the ground legs to keep the robot in balance.

$$\tan\varphi = (a+b)/L \tag{1}$$

$$B = R/sin\varphi \tag{2}$$

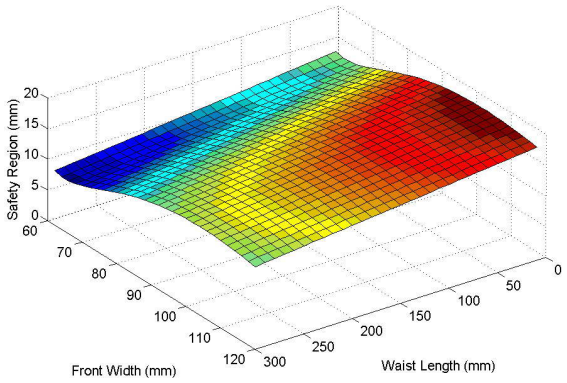

Fig. 3. The safety region for varying waist length, front, and rear width.

where a is the front, b is the rear leg width, R is the radius of the foot, B is the vertical distance between safety region lines, and L is the waist length. When the robot is stationary, as long as CG is in the SR, robot does not fall aside when two feet are aloft considering a quasitatic motion. However, when the robot moves, the CG moves a distance forward due to the rotation of the links, where θ is the angle of the front foot rotation and s is the step size of the CG.

$$s = a\sin\theta \tag{3}$$

Increasing the step size concludes decreasing the safety region with the amount of CG shift, s. It is obvious that if θ, during walking, gets smaller and the foot diameter gets bigger, maintaining the balance becomes easier. In other words, the safety region increases. The lengths a and b should be selected very carefully in order to make the CG lies on the intersection of centerline that connects front and rear leg centers and the line that connects rear and front waist motors. The main aim behind this idea is overlapping the CG point and SR center to maximize the usage of the SR when the robot steps forward and backward. The safety region is calculated for varying leg widths and waist lengths as shown in Fig. 3.

B. Climbing Analysis

Unlike ground walking, the projection of the CG shifts backward during climbing. This shift, ΔS, is related with the inclination, α, and CG height, h, of the robot.

$$\Delta S = h\tan\alpha \tag{4}$$

In addition, CG shifts sideways with the side slope, β, when Geckobot is walking across a slope. The CG height and dimensions of the robot directly affect the amount of side-shift as shown in Fig. 4. Due to the shift, safety region decreases with the amount of loss (ΔL). Side shift (S_s) can be expressed as

$$S_s = h\tan\beta \tag{5}$$

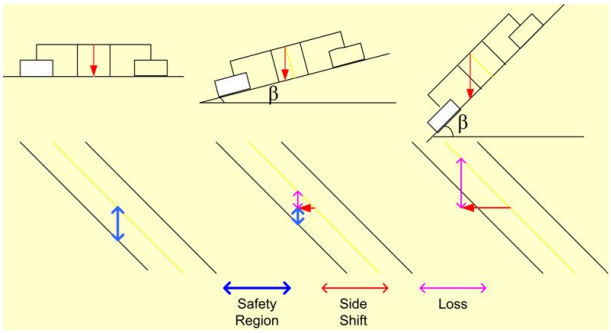

Fig. 4. Safety region shift during side-walking. (front view of the Geckobot)

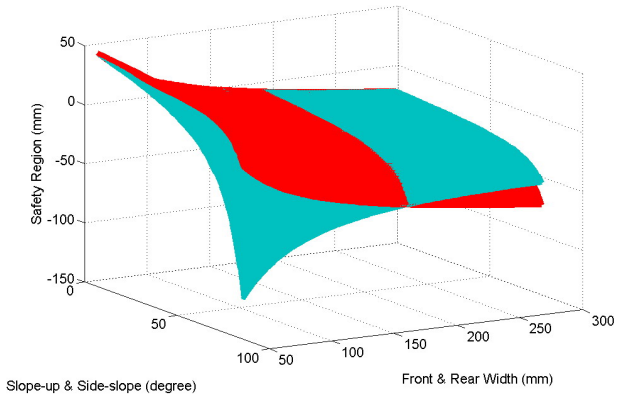

Fig. 5. Width optimization of the Geckobot to maximize the safety region.

and loss of the safety region can be expressed as

$$L_s = S_s/tan\varphi \tag{6}$$

In order to find the optimum width of the legs, climbing both up and across a slope are analyzed. First, the waist length of the robot is taken arbitrarily and the leg width was taken as a variable between 50 mm, and 300 mm for both side-walking and slope-up climbing to obtain a 3-D safety region. After combining these graphs into the same plot, an intersection line is observed as shown in Fig. 5. This line indicates the optimum width of the front and rear legs for a given waist length. If any other width is chosen, the performance of the side-walking might be increased but slope-up climbing performance is diminished or vice versa.

In Fig. 6, the force distribution during side walking is shown. F_{dx} and F_{ux} are the normal forces underneath the toes during side-walking.

$$F_{ux} = (mg\cos\beta - \sin\beta h)/2a \tag{7}$$

$$F_{dx} = mg\cos\beta - F_{ux} \tag{8}$$

A tail is one of the most important limbs for climbing animals and robots. There are some benefits of having a tail while climbing, such as; holding onto supports, maintaining balance and moving from one place to another, However, the main aim of having a tail in this paper is preloading. If some slope-up climbing angle is exceeded, the front toes detach from

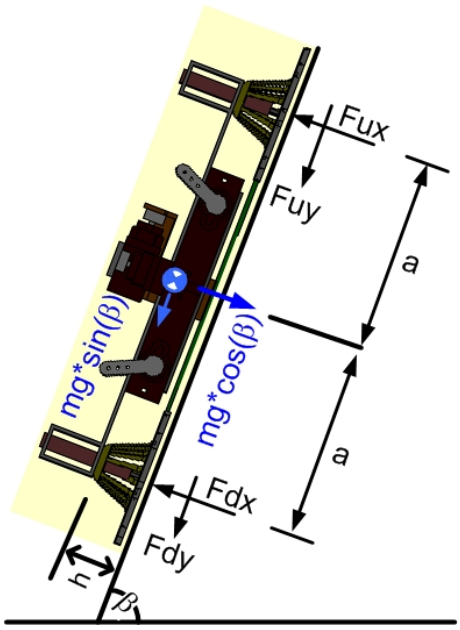

Fig. 6. Geckobot's force distributions during side-walking

the surface due to the moment about the rear legs caused by the CG. A tail is added to the system in order to transfer some load from the rear toes to the front toes increasing the maximum slope the robot can climb. To sum up, pressing against the surface with a tail increases the normal force on the front toes leading secure climbing. When Geckobot is climbing at $90\,^{\circ}$, at least 50 mN adhesion force is needed to keep the front toes on the surface without a tail as seen in Fig. 7. However, with the aid of the tail, the adhesion force needed can be decreased by preloading the tail. Fig. 8 shows the forces that act on Geckobot's toes and tail. F_{tx} can be assumed zero since the friction coefficient of the tail is very small and the preload on the tail is not more than $60mN$. F_{ty} is the tail preload and can be controlled by rotating the tail servo arm. Normal force under the rear toe becomes

$$F_{ry} = (mg\cos\alpha L_1 + mg\sin\alpha h - F_{ty}(L_1+L_2+L_3))/(L_1+L_2) \tag{9}$$

The normal force under the front toe turns out to be

$$F_{fy} = mg\cos\alpha - F_{ty} - F_{ry} \tag{10}$$

Climbing is achieved if normal force on the pad multiplied by coefficient of friction is bigger then the total force which pulls the robot downward parallel to the surface. If there are two components connected to each other and they have the same coefficient of friction constant, the one that has lesser amount of normal force slides first down if pulling down forces are equal, and may cause the other component to slide as well. For this reason, rear and front normal forces has to be as close as possible for better climbing. As a conclusion, the tail motor should push against the surface at just the right amount that the front and rear toes normal forces become equal at any time and any slope for stable climbing. This is because,

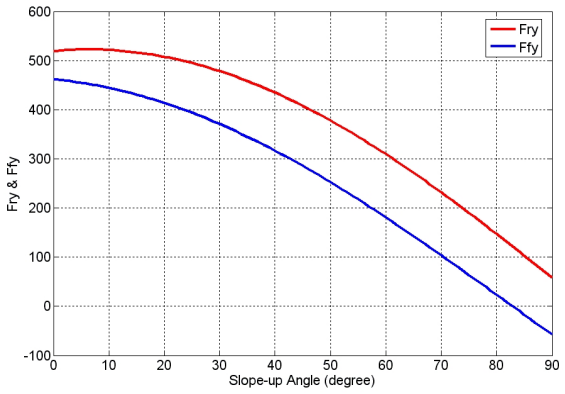

Fig. 7. Geckobot's force distribution without a tail during a slope-up climbing.

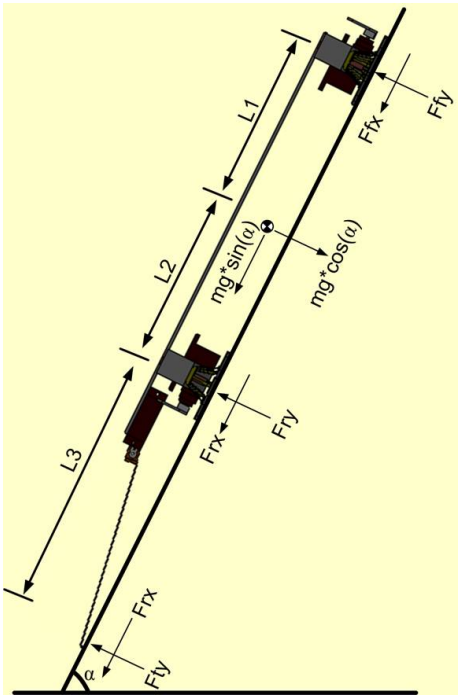

Fig. 8. Force distributions during a slope-up climbing.

although it is a four-bar mechanism, two actuators should be used to share climbing forces. In other words, the rear motor pushes and the front motor pulls the robot up. However, not proper synchronization of waist motors may result in a foot slip or inner torque accumulation and increasing instability. Synchronization is realized by using kinematic analysis of the Geckobot as shown in Fig. 9 for a given specific dimensions. From kinematics, it is found out that when the front motor rotates to a specific degree, there is just one correct position for the rear motor due to the single DOF as shown in Fig. 10.

$$be^{i\theta_3} + we^{i\theta_2} + ae^{i\theta_1} = |AD| \tag{11}$$

$$b\cos\theta_3 + a\cos\theta_1 = w - w\cos\theta_2 \tag{12}$$

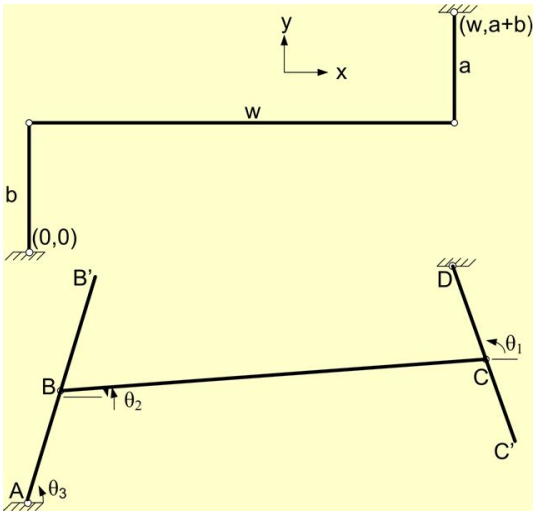

Fig. 9. Kinematic diagram of the Geckobot.

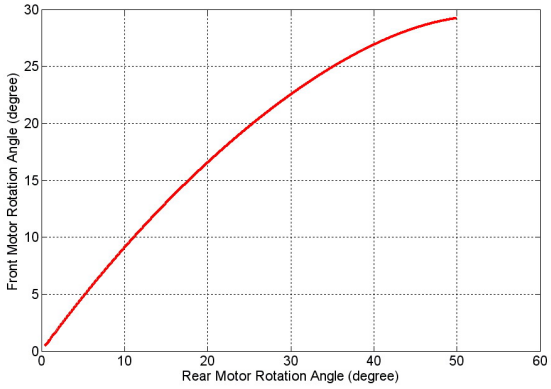

Fig. 10. Relationship of the rear and front motor rotations.

$$b\sin\theta_3 + a\sin\theta_1 = a + b - wsin\theta_2 \tag{13}$$

where, θ's are the angles between the links and arbitrarily chosen horizontal direction as shown, w is the waist length, and $|AD|$ is the vectorial distance between point A and D. The rear motor rotation angle is $(180 - \theta_3 + \theta_2)$ and, the front motor rotation angle is $(\theta_1 - \theta_2)$ and both of them can be controlled. To make the front and rear normal forces equal, tail normal force versus climbing angle versus normal force underneath the toes is drawn in 3-D mesh graph as shown in Fig. 11. The intersection of the front and rear preload surfaces give the force of the tail. A cubic equation is fitted to the intersection curve. Practically, the slope can be detected using an accelerometer, and put into the equation to determine the required normal force needed on the tail as shown in Fig. 12.

For accurate and precise preloading, the position of the tail must be controlled. To accomplish this, a servomotor should be chosen for actuation. If a tail is machined from a stiff material, very small rotation of the servomotor will create a large preload force on the tail, which is undesirable. Instead, a relatively compliant material should be used to get good

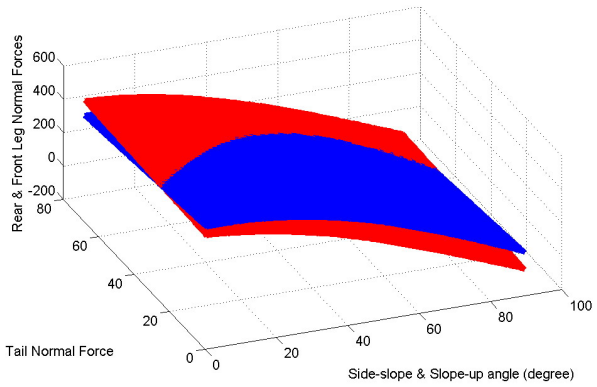

Fig. 11. The rear and front leg normal force for varying tail normal force and slope-up angle.

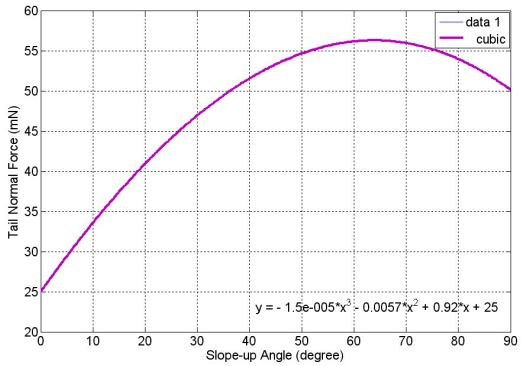

Fig. 12. Tail preload equation for varying slope.

resolution out of the servo rotation.

C. Steering

Steering is realized by controlling two servomotors on the four-bar mechanism separately when the rear feet are aloft. While the robot is walking, two motors rotate in a synchronized manner. To initialize steering, Geckobot's tail presses hard enough against the ground to cause hind feet detachment off the ground. Then, the front motor rotates the whole body to the desired position while the tail is sliding. Meanwhile, the back motor adjusts itself to the right angle for the next step synchronization.

D. Peeling Mechanism

The peeling mechanism is very crucial for climbing robots for power-efficient detachment as seen in geckos. For instance, to remove an ordinary piece of tape from an item, if pulled perpendicular to the surface from the center, a relatively high force would be required. However, if it is peeled starting from one side, it would come off very easily. Like the tape example, the Geckobot has to do peeling while climbing in order to minimize the foot detaching force.

The mechanism of the peeling system can be seen in Fig. 13. When one of the foot motor is energized, due to the rotation

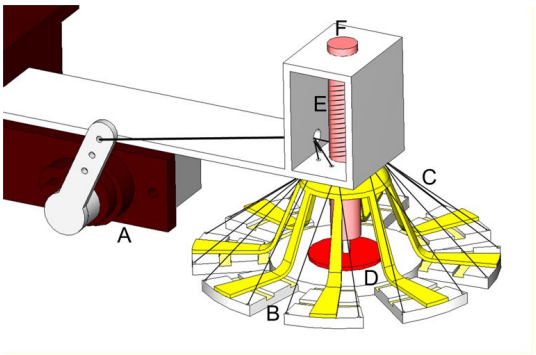

Fig. 13. CAD design of the peeling mechanism. A: Servomotor, B: Adhesive pads, C: Strings, D: Revolute joint, E: Spring, F: Cylindrical rod

and displacement of the servo arm, all strings and the adhesive Polydimethyl siloxane (PDMS) elastomer surfaces are pulled. Then starting from the edge, the PDMS starts to deflect and peels off. There is a compression spring on the shaft so when the pulling force exceeds the deflection threshold of the spring, foot starts to move up. Reattachment to the ground is accomplished by rotating the servo arm to its original position. Since compression springs are used, they push the whole mechanism back to its original position.

III. PROTOTYPE

A. Body Materials and Circuitry

The chassis of the Geckobot was built from Delrin®. The robot was equipped with seven servomotors (GWS Pico STD), four used for lifting the robotic legs, two for robot locomotion, and one for the active tail. The output torque of the servomotors is 70 Nmm when 5 V is applied. PDMS is used as the dry adhesive elastomer material. PDMS adhesion pressure for various preloads is displayed in Fig. 14. On top of the PDMS layer, a very thin stainless steel is used for both fixing the strings securely and giving the spring back behavior to the whole foot after peeling. Strings pass between the PDMS layer and the stainless steel sheet then they go out of the mold from the edges and are connected to the servomotors with the aid of superglue. In the four-bar mechanism, there is a revolute joint on top of the PDMS layer, half buried into the PDMS. All strings are passed through the same hole, when motor is actuated, it is thereby guaranteed that all strings and deflected PDMS move the same distance.

To find the force output of the tail tip from a given servo rotation angle, small beam deflection theory is used. After some calculations, tail dimensions are decided to be 0.66 mm thick, 10 mm wide and 100 mm long delrin material. When the motor rotates $14\,^{\circ}$, the tail preload reaches 50 mN, which is the desired theoretical preload.

$$I = wt^3/12 \tag{14}$$

$$\theta_t = ML_t/3EI \tag{15}$$

where, I is the moment of inertia, w is the width and t is the thickness of the tail, θ_t is the servo motor as well as base of the

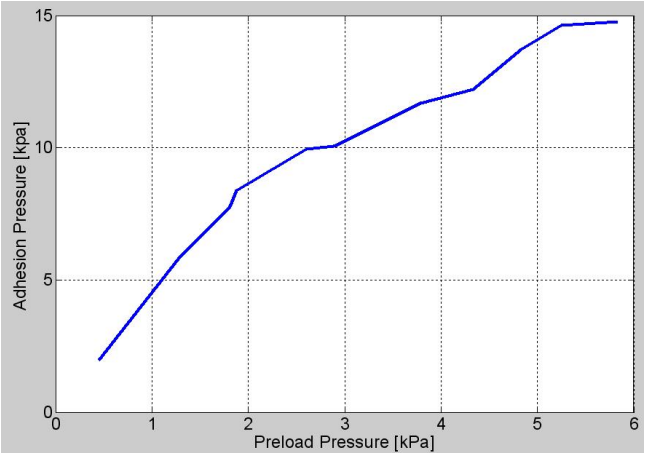

Fig. 14. Preload vs adhesion graph of a PDMS.

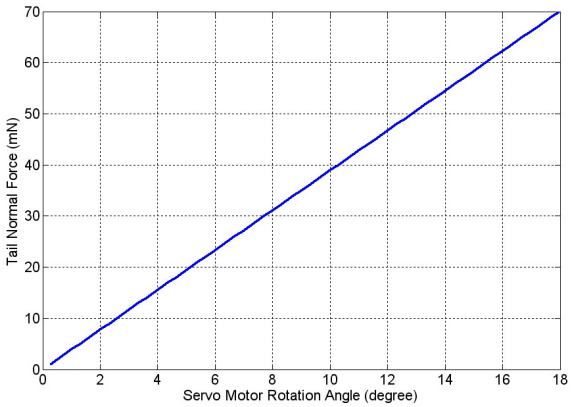

Fig. 15. Tail normal force for varying servomotor rotation angle.

tail rotation angle and L_t the tail length. The Young's modulus of the delrin material is taken as 3 MPa. By using (15), tail normal force versus servomotor rotation angle is drawn as illustrated in Fig. 15.

A compact on-board circuit is placed on the waist. This circuit expands the functionalities of the robot by adding modules such as wireless infrared (IR) communication, obstacle avoidance, serial communication, and in-circuit serial programming (ICSP) compatibility. The robot can be controlled via IR over RC5 protocol or serial communication over RS232. The IR proximity sensors allow the robot to avoid obstacles and steer away from them. The motors are driven by a microcontroller, which also runs the main program. A three-axis accelerometer is used to sense orientation and control the active tail.

B. Software

The robot's kinematic and dynamic analysis are mainly carried out with a MATLAB Simulink model. The main parts of the robot were represented with SimMechanics blocks. The model can input its parameters (i.e. body dimension, PDMS constants, etc.) through a GUI interface and can display the results via dialog boxes, graphs, and an animation from Virtual Reality Toolbox. The tail option can also be selected in order

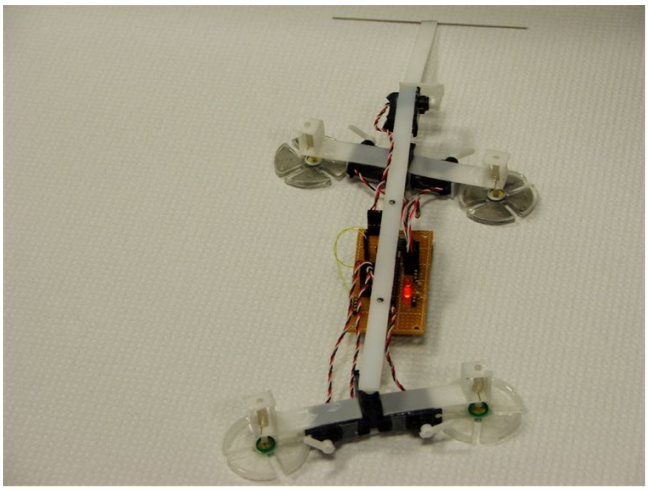

Fig. 16. Photo of the Geckobot as parts displayed in Fig.1

to compare the results with or without the tail. The model gradually increases the tilt of the surface. Meanwhile, code is checking for kinematic instability, dynamic imbalance, and the adhesion limits between the surface and the feet of the robot. When one of these checks fail, the simulation stops and the maximum tilt reached is displayed along with the graphs.

IV. EXPERIMENTS

The overall weight of the robot is 100 grams including the electronic board. The total length is 190 mm without the tail, width is 110 mm and tail is 100 mm as shown in Fig. 16. The distance between the front legs and the CG is 100 mm. During experiments, flat adhesives are used underneath the feet. The speed of the robot is 5 cm/s during walking on the ground. However, when climbing at higher angles, it is decreased to 1 cm/s due to stability reasons. The robot is slowed down to avoid attachment and detachment vibrations during climbing. Geckobot can climb up to 85° stably on Plexiglas surfaces as seen in Fig. 17. However, beyond this angle stability diminishes abruptly. Since Geckobot is mainly designed for slope-up climbing instead of side-walking, its length is longer than its width, which diminishes the robot's side-walking performances. Geckobot cannot walk sideways on a slope of more than 50°. Steering can be done effectively and very stably until 45°, as displayed in Fig. 18. The power consumption of the robot is around 1.4 Watts while climbing at 85° mainly due to the servomotors.

Experimental results of the tail preload force versus servomotor rotation angle is exactly matched with the theoretical calculations as showed in Fig. 15.

V. DISCUSSIONS

The performance of the robot depends on the chosen adhesive and peeling mechanism. The presented research opens a new avenue in the design of high performance miniature wall-climbing robots using an active tail and peeling mechanism with dry adhesives. Here, flat PDMS elastomer is chosen as a dry adhesive. Although PDMS is a stable material, it is

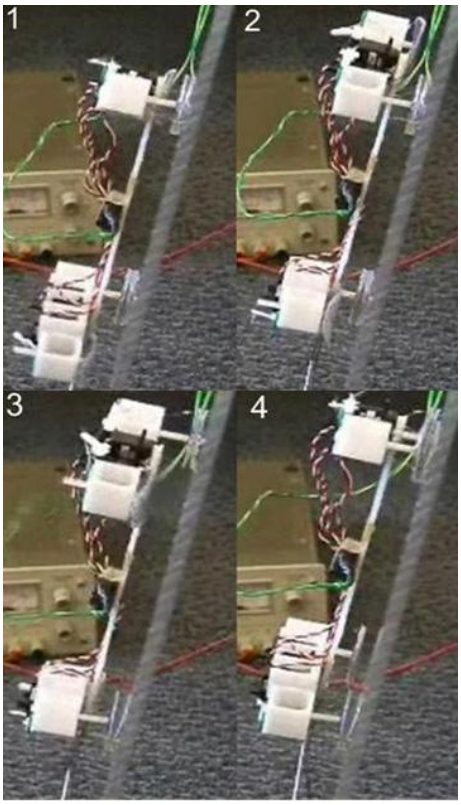

Fig. 17. Photo snapshots of the Geckobot climbing on an acrylic flat surface with 85° slope.

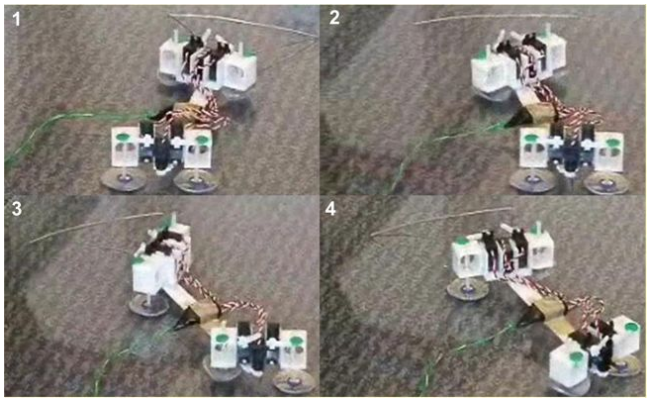

Fig. 18. Photo snapshots of the Geckobot steering on a horizontal surface.

degraded and contaminated by dust and dirt within the time. That is, after sometime it looses its adhesive characteristics and some properties. This problem would be improved using micro-patterned PDMS to have self-cleaning characteristic like geckos.

Since an open-loop control system is used on the tail mechanism, the robot does not control its tail through feedback from the system, potentially causing some problems during climbing. In addition, the Geckobot cannot peel very effectively due to the lack of molding techniques.

If the force calculations are realized again considering the same preload under the front and rear toes

$$F_{fy} = (mg\cos\alpha(L_3 + b) - \sin\alpha h)/(L_1 + L_2 + 2L_3) \quad (16)$$

$$F_{ux} = mg(\cos\beta - \sin\beta h)/(2a) \quad (17)$$

are derived for slope-up climbing and side-walking. It is seen that, for climbing steeper angles the lengths of the robot should be increased. However, tail length, L_3, is much more important than L_1 or L_2. For side-walking, the robot should be as wide as it can be. For both cases, Geckobot should be designed very light and very close to the ground.

VI. CONCLUSION

Miniature wall-climbing robots have a number of advantages over their larger counterparts. The miniature wall-climbing robot design presented in this paper overcomes challenges in climbing with dry adhesives, steering, peeling and active preloading of the tail. It demonstrates effective climbing behavior on inclined surfaces up to 85° at a speed of 1 cm/s. The robot design is demonstrated to be efficient, reliable, and robust. Unresolved issues with the current prototype include 90° surface climbing, obstacle avoidance, and autonomous navigation. These issues will be addressed in the next prototype, which is currently under development using new on-board electronics, sensors, and a camera.

REFERENCES

[1] L. Briones, P. Bustamante, and M. Serna, "ROBICEN: A wall-climbing pneumatic robot for inspection in nuclear power plants," *Robotics and Computer-Integrated Manufacturing* vol. 11, 287-292, 1994.

[2] Z. Xu and P. Ma, "A wall-climbing robot for labeling scale of oil tank's volume," *Robotica* vol. 20, 209-212, 2002.

[3] Z. Yanzeng, S. Hao, and W. Yan, "Wall-climbing robot with negative pressure sucker used for cleaning work, " *High Technology Letters* vol. 5, 85-88, 1999.

[4] L. Shuliang, Z. Yanzheng, G. Xueshan, X. Dianguo, and Wang Yan, "A wall-climbing robot with magnetic crawlers for sand-blasting," *Spray-Painting and Measurement High Technology Letters* vol. 10, 86-8, 2000.

[5] S. Tokioka, and S. Sakai, "Painting robot for wall surface," *Robot* vol. 65, 88-96, 1988.

[6] R.T. Pack, J.L. Christopher, and K. Kawamura, "A Rubbertuator-Based Structure-Climbing Inspection Robot," *Proceedings of the IEEE International Conference on Robotics and Automation*, pp. 1869-1874, 1997.

[7] A. Nagakubo and S. Hirose, "Walking and running of the quadruped wall-climbing robot," *Proceedings of the IEEE International Conference on Robotics and Automation*, pp. 1005-1012, 1994.

[8] H.R. Choi, S.M. Ryew, T.H. Kang, J.H. Lee, and H.M. Kim, "A wall climbing robot with closed link mechanism" *Proc. of the Intelligent Robotic Systems Conference*, pp. 2006-2011, vol. 3, 2000.

[9] L. Shuliang, Z. Yanzheng, G. Xueshan, X. Dianguo, and W. Yan, "A wall climbing robot with magnetic crawlers for sand-blasting. Spray-Painting and Measurement," *High Technology Letters*, pp 86-88, vol. 10, 2000.

[10] T. Bretl, T. Miller, S. Rock and J.C. Latombe, "Climbing Robots in Natural Terrain," *7th Int. Symp. on Artificial Intelligence, Robotics and Automation in Space*, Nara, Japan, May 2003.

[11] K. Autumn, Y. Liang, T. Hsieh, W, Zesch, W.P. Chan, T. Kenny, R. Fearing, and R.J. Full, "Adhesive force of a single Geckobot foot hair," *Nature*, 405, pp. 681-5, 08 June 2000.

[12] J.G. Cham, S.A. Bailey, and M.R. Cutkosky, "Robust dynamic locomotion through feedforward-preflex interaction," *CProc. of the ASME IMECE*, Orlando, Florida, November, 2000.